
Valence–Arousal Subspace in LLMs: Circular Emotion Geometry and Multi-Behavioral Control

Lihao Sun^{1,2†} Lewen Yan¹ Xiaoya Lu¹ Andrew Lee³ Jie Zhang¹ Jing Shao¹

Abstract

We present a method to identify a valence–arousal (VA) subspace within large language model representations. From 211k emotion-labeled texts, we derive emotion steering vectors, then learn VA axes as linear combinations of their top PCA components via ridge regression on the model’s self-reported valence–arousal scores. The resulting VA subspace exhibits circular geometry consistent with established models of human emotion perception. Projections along our recovered VA subspace correlate with human-crowdsourced VA ratings across 44k lexical items. Furthermore, steering generation along these axes produces monotonic shifts in the corresponding affective dimensions of model outputs. Steering along these directions also induces near-monotonic bidirectional control over refusal and sycophancy: increasing arousal decreases refusal and increases sycophancy, and vice versa. These effects replicate across Llama-3.1-8B, Qwen3-8B, and Qwen3-14B, demonstrating cross-architecture generality. We provide a mechanistic account for these effects and prior emotionally-framed controls: refusal-associated tokens (“I can’t,” “sorry”) occupy low-arousal, negative-valence regions, so VA steering directly modulates their emission probability.

1. Introduction

A growing body of work shows that emotionally framed prompting or activation steering influences large language model (LLM) behavior (Li et al., 2023; Konen et al., 2024; Reichman et al., 2025; Dong et al., 2025). Yet why such methods work—and when they fail—remains unclear.

One obstacle is conceptual. Work that studies such phenomena in LLMs typically treats discrete emotion categories—

anger, joy, fear—as fundamental units of analysis (Zhang et al., 2024; Tigges et al., 2024; del Arco et al., 2024; Konen et al., 2024; Dong et al., 2025). To find a common basis for comparison, a growing trend borrows from human psychology the two-dimensional framework of valence (pleasure–displeasure) and arousal (activation–deactivation) (Ishikawa & Yoshino, 2025; Felix-Pena et al., 2025). In practice, these dimensions are often equated with categorical labels or used merely as evaluation metrics. Though yielding insights, this discreteness-driven perspective forgoes explanatory power that the original distinction affords.

In the psychological tradition from which these constructs originate, valence and arousal (VA) do not define emotions themselves but rather core affect—a continuous experiential substrate from which discrete emotions emerge (Russell, 1980; 2003). Emotions arise when core affect is attributed to a cause and labeled with a culturally available category: a pleasant, high-arousal state, attributed to an unexpected gift, becomes surprise or excitement. We invoke this distinction not as a claim about LLM phenomenology, but as a modeling choice: continuous dimensions and discrete labels play different explanatory roles and should not be conflated.

In this work, we treat categorical labels and VA axes as separate structures and demonstrate the insights this decoupling affords. At the level of model representations, this conceptual shift also motivates a methodological one. Many existing steering-vector methods construct directions via contrastive differences (e.g., mean activation differences over paired examples) (Panickssery et al., 2024). While effective, these directions can be brittle—often requiring careful tuning across prompts, layers, or behaviors, and may not directly transfer without additional alignment or mapping (Tan et al., 2025; Braun et al., 2025; Oozeer et al., 2025). We show that decomposing emotion steering vectors into a low-dimensional VA subspace yields shared structure that generalizes across multiple downstream behaviors, suggesting a more reusable control basis than single-task contrastive directions.

Concretely, our approach proceeds as follows. From 211,225 emotion-labeled text samples, we derive emotion steering vectors via mean-difference contrasts between emotion-labeled and neutral examples (Demszky et al.,

¹Shanghai AI Lab ²University of Chicago ³Harvard University.
Correspondence to: Jing Shao <shaojing@pjlab.org.cn>.

† Work done using resources from Shanghai AI Lab.

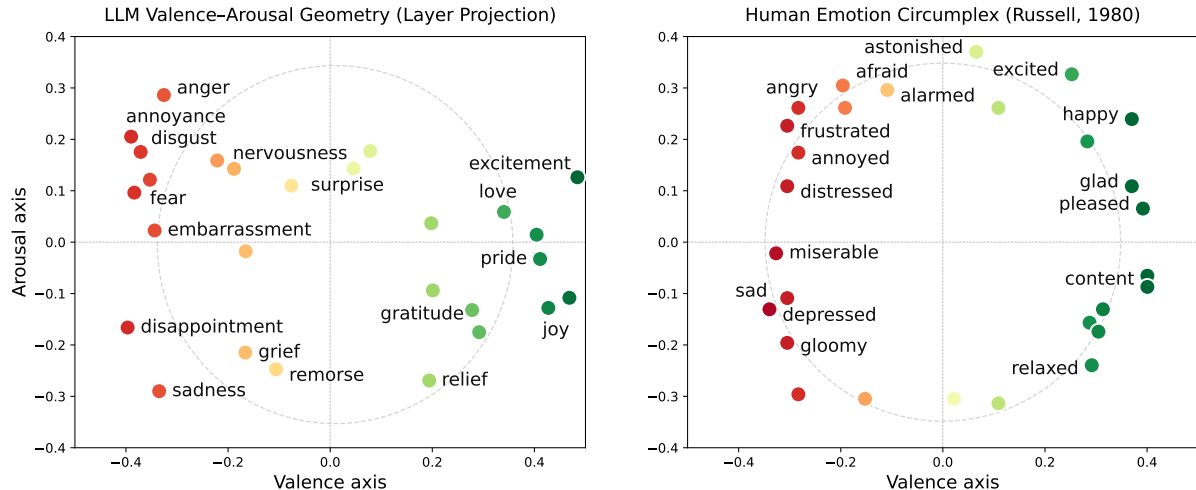


Figure 1. Emotion steering vectors projected onto the VA subspace at layer 31, colored by valence. Gray circle: algebraic least-squares fit. The circular arrangement is analogous to circumplex model of affect in human psychology (Russell, 1980).

2020). We then obtain the model’s self-reported VA ratings for each emotion category and learn VA subspaces as linear combinations of principal components of the emotion vectors, optimized via ridge regression to recover these self-reported scores. When projected onto the learned VA subspace, the emotion vectors exhibit circular geometry analogous to the circumplex model from human emotion perception (Russell, 1980), as shown in Figure 1.

To validate the learned subspaces, we first show that VA scores obtained from projections on learned subspaces correlate with human-crowdsourced VA ratings across 44,728 lexical items (Mohammad, 2025). Second, we demonstrate that steering generation on open-ended prompts along these axes produces monotonic shifts in the corresponding affective dimensions of model outputs, as measured by sentiment and a pre-trained BERT model for VAD scoring (Hutto & Gilbert, 2014; RobroKools, 2022). These results provide evidence that the identified axes afford VA-specific control over the affective properties of model responses.

To further explore the relationship between VA subspaces and downstream behaviors, we find VA axes afford near-monotonic control over refusal and sycophancy: increasing arousal decreases refusal rates and increases sycophancy, while decreasing arousal produces the opposite pattern. Random directions yield no or much weaker effects. These effects replicate on Llama 3.1 8B, Qwen3-8B and Qwen3-14B, confirming cross-architecture generality. Surprisingly, the VA subspaces are nearly orthogonal to refusal directions derived via contrastive mean difference (Arditi et al., 2024), yet both yield monotonic control in our settings.

Based on these observations, we propose a unifying mechanistic explanation for why our approach and prior emotionally-framed methods successfully control model be-

havior: lexical mediation. Refusal-associated tokens (e.g., “can’t,” “sorry”) and compliance-associated tokens (e.g., “sure,” “Here”) occupy distinct regions in VA space, so shifting VA coordinates changes the likelihood of emitting such markers, thereby modulating downstream behavior. We further show that prior emotionally-framed prompting methods induce corresponding shifts in the VA subspace, suggesting a similar underlying mechanism.

Taken together, our work advances understanding of affective phenomena in LLMs by motivating a conceptual separation between discrete emotion labels and continuous valence–arousal dimensions, demonstrating how this two-level perspective yields meaningful insights. Specifically, we identify a 2-dimensional VA subspace and provide evidence that emotion vectors are systematically organized within this geometry. From an interpretability standpoint, we present principal-component-based decomposition of emotion steering vectors into interpretable subspaces as a complementary approach to task-specific steering, exposing shared structure that generalizes across behaviors toward domain-agnostic control. Finally, we offer a unifying mechanistic account—lexical mediation—that explains why emotion-based prompting and emotion steering influence model behavior. We do not claim that VA is the unique pathway; rather, we propose it as one plausible explanation for why emotion-based controls work in LLMs.

2. Related Work

Geometry of representations in LLMs. A growing body of work seeks to discover the linear and low-dimensional structure of how features are arranged in activation space in LLMs. Most of the work is 1D, a single linear direction whose sign or magnitude predicts or controls a be-

havior (Turner et al., 2024; Panickssery et al., 2024; Sun et al., 2025; Lee et al., 2025a). Prior work has also shown that LLMs linearly represent sentiment or polarity (Tigges et al., 2023). By contrast, 2D geometries in LLMs are less commonly characterized; notable studies include low-dimensional structure for space/time (Gurnee & Tegmark, 2024) and understanding trigonometry operations in 2D circles (Nanda et al., 2023). We add to this smaller set by demonstrating that emotion steering vectors are organized by a 2D VA geometry with behavioral consequences that a polarity-only account would not predict: the axes transfer differently to refusal and sycophancy, with arousal providing clean monotonic control.

Emotionally Framed Analysis and Control in LLMs. Appending emotionally framed phrases to prompts has been shown to influence LLM behavior and improve task performance across domains (Li et al., 2023; 2024). Existing explanations have attributed these effects to attention mechanisms, surface cues, or biases toward positive or negative affect (Wang et al., 2024; Zhou et al., 2024). We provide a unifying, top-down mechanistic account that links emotionally framed behaviors across representation-level geometry, unembedding structure, and neuron-level analyses. Concurrent work by Anthropic (Sofroniew et al., 2026) identifies discrete emotion concept representations in Claude Sonnet 4.5 that influence downstream behaviors; our work complements theirs by decomposing such categorical representations into a continuous 2D valence–arousal substrate and characterizing the geometric structure that organizes them.

Activation Steering. Activation steering enables training-free behavioral control by manipulating internal representations (Zou et al., 2025), but typically relies on task-specific contrastive vectors for each desired behavior (Turner et al., 2024; Qian et al., 2024; Lee et al., 2025b). Notably, emotions have been shown to correspond to linear directions in activation space (Tigges et al., 2023; 2024). In this work, we present an approach of principal-components-based decomposition into subspaces, which complements the mainstream contrastive task-specific approach.

3. Identifying Valence and Arousal Subspaces

We decompose emotion steering vectors to identify underlying VA subspaces. Our approach proceeds in three stages: (1) extracting emotion directions via mean-difference contrasts, (2) eliciting model self-reported VA coordinates for each emotion label, and (3) learning VA axes as linear combinations of principal components via ridge regression. Here, we present results on Llama 3.1-8B-Instruct (Meta, 2024) and replicate on Qwen3-8B and Qwen3-14B (Yang et al., 2025) to validate cross-architecture generality.

Emotion Steering Vectors. Using Llama 3.1-8B-Instruct

(Meta, 2024), we derive emotion steering vectors using contrastive means (Tigges et al., 2023; Panickssery et al., 2024; Dong et al., 2025). We use GoEmotions (Demszky et al., 2020), which comprises 211,225 text samples annotated with 27 emotion labels plus a neutral class. We only retain examples annotated with exactly one emotion. For each emotion category e , we extract the last-token hidden state of each sample at each layer. The steering vector at layer ℓ is

$$\mathbf{v}_e^{(\ell)} = \frac{1}{|D_e|} \sum_{x \in D_e} \mathbf{h}^{(\ell)}(x) - \frac{1}{|D_{\text{neutral}}|} \sum_{x \in D_{\text{neutral}}} \mathbf{h}^{(\ell)}(x) \quad (1)$$

where $\mathbf{h}^{(\ell)}(x) \in \mathbb{R}^H$ denotes the last-token hidden state at layer ℓ for input x ; D_e and D_{neutral} are the sets of single-label examples for emotion e and the neutral category.

Next, we obtain VA scores by prompting the model to self-report the valence and arousal for each emotion label, averaging across three prompt templates for robustness (see Appendix A.1). We operationalize both dimensions as continuous values in the range $[-1, +1]$: valence spans from extremely unpleasant (-1) to extremely pleasant ($+1$), and arousal spans from very calm (-1) to very activated ($+1$), with 0 denoting neutrality on each axis.

Decomposing Steering Vectors into Subspaces. For each layer ℓ , we analyze the emotion steering vectors $\mathbf{V}^{(\ell)} \in \mathbb{R}^{K \times H}$ independently. We first mean-center the vectors and apply principal component analysis to obtain a low-rank basis. Let $\mathbf{U}_k \in \mathbb{R}^{H \times k}$ denote the top k principal component directions, and let $\mathbf{Z} \in \mathbb{R}^{K \times k}$ denote the projection of the centered emotion vectors onto these components (i.e., the PC scores). We then fit ridge regression models to recover the self-reported valence and arousal scores:

$$\hat{\beta}_V = \arg \min_{\beta} \|\mathbf{Z}\beta - \tilde{\mathbf{y}}_V\|^2 + \lambda \|\beta\|^2 \quad (2)$$

where $\tilde{\mathbf{y}}_V$ denotes the mean-centered valence ratings, and analogously for arousal. The learned coefficients $\hat{\beta}_V \in \mathbb{R}^k$ define the valence axis as a linear combination of principal components. The corresponding direction in the original activation space is given by $\mathbf{w}_V = \mathbf{U}_k \hat{\beta}_V$, normalized to unit length. With Gram–Schmidt orthogonalization, we ensure the valence and arousal axes are orthonormal.

Figure 2 reports recovery performance across layers. Using PC1 alone, valence is well captured ($r = 0.89$ at layer 4), with correlations exceeding 0.80 across most middle layers—indicating valence aligns with the principal axis of variation among emotion steering vectors. Arousal, by contrast, is poorly captured by any single principal component ($r = 0.54$). Ridge regression over multiple components improves both: valence reaches $r = 0.97$ and arousal reaches $r = 0.87$. This asymmetry implies valence constitutes the dominant dimension of emotion steering vectors, while arousal is distributed across secondary components.

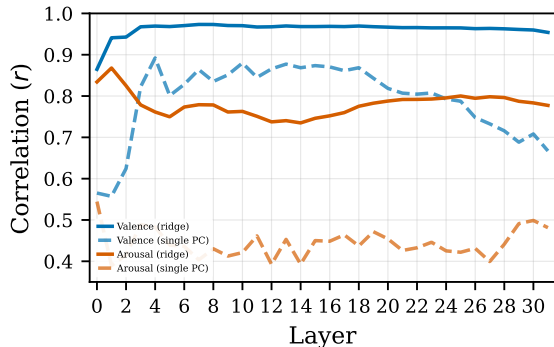


Figure 2. Recovery of self-reported VA scores via correlation with learned subspace projections across layers. Solid lines: ridge regression over multiple PCs; dashed lines: best single PC.

Circular Geometry of Emotion Representations. Projecting emotion steering vectors onto the learned VA subspace reveals a circular arrangement analogous to Russell’s circumplex model found in human psychology (Russell, 1980). Qualitatively, positive emotions (*joy*, *gratitude*) oppose negative ones (*sadness*, *grief*) along valence, while high-arousal states (*excitement*, *anger*) separate from low-arousal states (*relief*, *sadness*) along the orthogonal axis (Figure 1). To quantify this structure, we fit circles to the projected coordinates using algebraic least squares, minimizing squared radial residuals. We report *circularity*—the ratio of mean to standard deviation of distances from the fitted center—where higher values indicate tighter circular arrangement. Figure 1 shows the fit at layer 31, where circularity reaches 3.17 with normalized RMSE of 0.30. Similar circular geometry is observed across layers. We note that some degree of circular organization is expected given supervision targets that themselves follow a circumplex arrangement. The evidence for genuine internal structure comes not from this identification step alone, but from the subsequent validation (Section 4) and intervention (Section 5) results. Notably, concurrent work by Sofroniew et al. (2026) recovers the same circumplex-consistent geometry in Claude Sonnet 4.5 using an independent pipeline (synthetic story generation, mean activations, PCA projection), with their PC1 correlating with human valence at $r = 0.81$ and PC2 with arousal at $r = 0.66$ —paralleling our finding that valence aligns with PC1 while arousal requires multiple components.

Cross-Model Generalization. To assess whether the VA subspace is specific to Llama or reflects a more general property, we apply the same extraction and fitting pipeline to Qwen3-8B and Qwen3-14B. Table 1 reports the key metrics. The VA subspace consistently emerges across architectures: circle radii (0.37, 0.37, 0.39), VA projection magnitudes (0.35, 0.34, 0.36), and recovery correlations are all comparable, confirming that the geometric structure and V–A recovery asymmetry are consistent across models, with arousal systematically harder to recover than valence.

Table 1. Cross-model VA subspace identification. Circularity, recovery correlations, circle radius, and VA projection magnitude are comparable across architectures.

	Llama 3.1-8B	Qwen3 8B	Qwen3 14B
Circularity	4.08 (L5)	3.13 (L6)	2.76 (L24)
V recovery (r)	0.97	0.96	0.97
A recovery (r)	0.87	0.79	0.81
Circle radius	0.37	0.37	0.39
VA proj. mag.	0.35	0.34	0.36

Human-Supervised Validation of Self-Reported Axes.

We also refit the subspace using human NRC-VAD ratings (Mohammad, 2025) in place of model self-reports as supervision targets. This yields stronger arousal recovery in all three models (Llama: 0.87 \rightarrow 0.95; Qwen3-8B: 0.79 \rightarrow 0.83; Qwen3-14B: 0.81 \rightarrow 0.87), while valence recovery remains consistently high. The valence directions learned from human supervision and from self-reports are also closely aligned, with $|\cos| > 0.9$ at 100% of layers in all three models. At the lexical level, model self-reports correlate substantially with human NRC-VAD ratings across 44,728 words ($r = 0.80$ – 0.86 for valence; $r = 0.44$ – 0.55 for arousal), and cross-model agreement on the 27 emotion labels reaches $r = 0.95$ for valence between Llama and Qwen3-8B. Together with the concurrent independent recovery reported by Sofroniew et al. (2026), these results support the robustness of the recovered VA structure across supervision sources, models, and analysis pipelines.

4. Validation of VA Subspaces

Using VA subspaces identified in Section 3, we now address two questions: (1) do the learned VA axes correspond to human affective judgments, and (2) can steering along these axes produce controlled changes in model behavior?

4.1. Correlation with Human-Annotated VAD Lexicons

To assess whether the learned VA subspaces align with human affective perception, we project words from the NRC-VAD Lexicon (Mohammad, 2025)—containing human ratings for 44,728 English words—onto VA subspaces and compute correlations with the human norms.

For each word, we extract the model’s hidden state at the last timestep and project onto layer-specific VA axes using the same centering and projection procedure as in Section 3: $v_{\text{proj}} = (\mathbf{h} - \boldsymbol{\mu}) \cdot \mathbf{v}_{\text{dir}}$ and $a_{\text{proj}} = (\mathbf{h} - \boldsymbol{\mu}) \cdot \mathbf{a}_{\text{dir}}$, where $\boldsymbol{\mu}$ is the mean activation computed during subspace fitting.

Valence projections correlate strongly with human ratings, reaching $r = 0.71$ ($\rho = 0.69$) at layer 6. This is substantial given that we compare single-word activations against human judgments that may incorporate implicit contextual

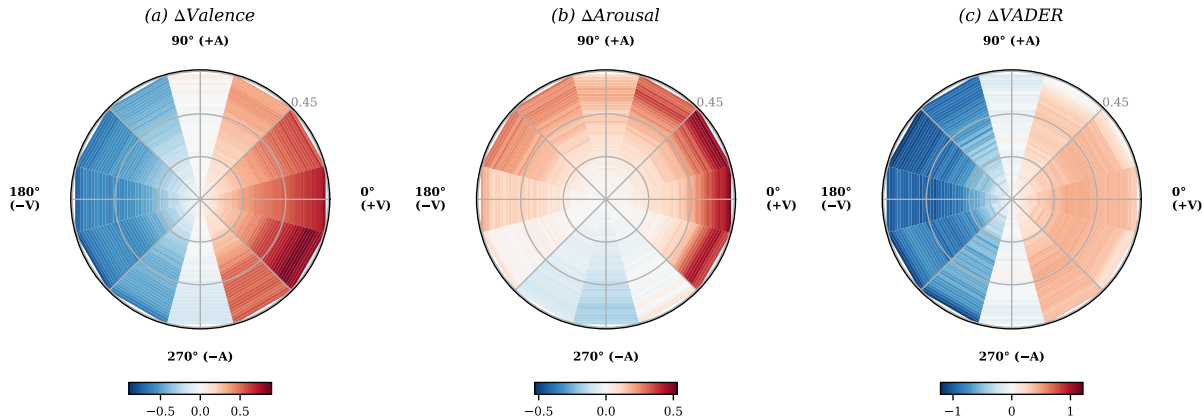


Figure 3. Radial heatmaps showing the effect of VA steering on open-ended generation. Each panel displays the change relative to unsteered baseline as a function of steering direction (angle) and strength (radius, $\alpha \in [0.01, 0.45]$). Cardinal directions: $0^\circ = +V$, $90^\circ = +A$, $180^\circ = -V$, $270^\circ = -A$. (a) Valence change (VAD-BERT). (b) Arousal change (VAD-BERT). (c) Sentiment change (VADER). The horizontal gradient in (a) and vertical gradient in (b) confirm the learned subspace enables controllable, geometrically predictable modulation of affect.

associations. Arousal projections show weaker correlations, peaking at $r = 0.23$ ($\rho = 0.22$) at layer 7. This asymmetry, where valence is far more predictable than arousal from decontextualized words, aligns with prior findings in affective computing (Sneffjella & Kuperman, 2016; Delatorre et al., 2019; Bruyne et al., 2021; Mendes & Martins, 2023): arousal depends heavily on situational context that isolated words cannot provide, whereas valence is more stably encoded in lexical semantics. Both correlations are highly significant ($p < 10^{-16}$), confirming that our VA subspace captures human-interpretable affective dimensions.

4.2. Controllable Generation via VA Steering

To test the interventional power of the VA subspaces, we apply activation steering on open-ended prompts and measure the changes in valence, arousal, and sentiment scores.

Steering method. Given steering direction $\mathbf{d} \in \mathbb{R}^{L \times H}$ (one vector per layer) and strength α , we add $\alpha \cdot \mathbf{d}_\ell$ to the hidden state at every token position in layer ℓ during generation. We steer along 12 angular directions in VA space ($0^\circ, 30^\circ, \dots, 330^\circ$), where 0° aligns with positive valence and 90° with positive arousal, at 45 steering strengths ($\alpha \in [0.01, 0.45]$). All generations use greedy decoding.

Prompt design. We evaluate on 130 prompts (adapted and expanded from Konen et al. (2024)) structured in three tiers: (1) emotionally neutral scenarios describing everyday actions and interpersonal moments without affective language (e.g., “someone opens a letter,” “a boss asks an employee”), (2) story continuations with open-ended beginnings, and (3) subjective prompts adapted from Konen et al. (2024) plus factual questions. This tiered, neutral design isolates steering effects from prompt-induced emotion while testing generalization across response lengths and genres. See

Appendix B for the full prompt list.

Scoring. Generated responses are scored by two independent systems. VADER (Hutto & Gilbert, 2014) is a lexicon-based sentiment analyzer that outputs a compound score in $[-1, +1]$, where -1 indicates maximally negative sentiment and $+1$ maximally positive. VAD-BERT (Buechel & Hahn, 2022; RobroKools, 2022) is a BERT-based regressor trained on the EmoBank corpus to predict valence and arousal scores on a 1–5 scale, where 1 indicates low and 5 high intensity for each dimension. Using both systems provides complementary validation: VADER captures lexical sentiment while VAD-BERT provides dimensional VA ratings aligned with our theoretical framework.

Results. Figure 3 shows the change in each metric relative to unsteered baseline, as a function of steering direction (angle) and strength (radius). Baseline generations occupy a near-neutral region of affect space (mean valence = 3.05, mean arousal = 3.29 on the 1–5 VAD-BERT scale), providing room for bidirectional modulation.

Steering along the valence axis produces strong, monotonic, and symmetric effects (Figure 3a): the 0° direction yields $\Delta V = +0.75$ at maximum strength while 180° produces $\Delta V = -0.73$, spanning 1.5 points on the VAD-BERT scale. VADER sentiment closely tracks this pattern (Figure 3c), providing independent confirmation that the learned V direction captures human-interpretable positive–negative affect.

Steering along the arousal axis produces directionally correct effects (Figure 3b): the 90° direction increases arousal ($\Delta A = +0.50$), while 270° yields decreases ($\Delta A = -0.16$). We also observe collateral arousal increases from valence steering: both $+V$ (0° : $\Delta A = +0.49$) and $-V$ (180° : $\Delta A = +0.22$) elevate arousal. This suggests a property of natural text rather than subspace geometry: highly

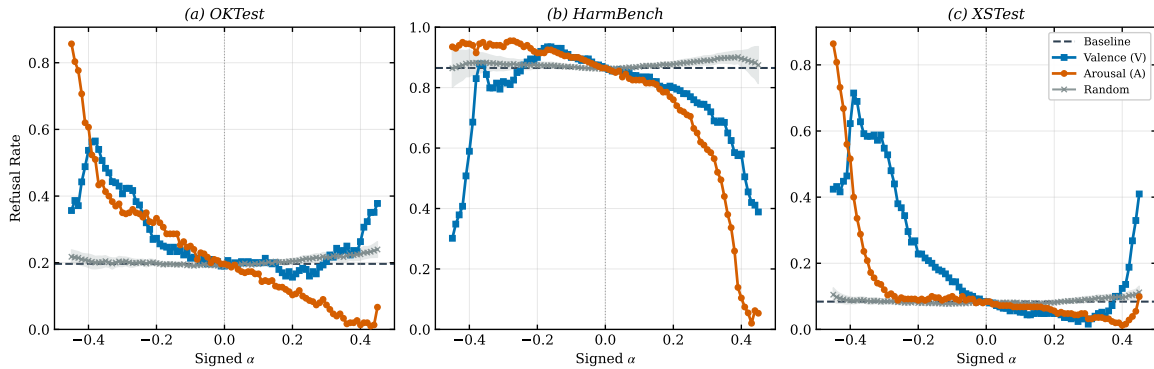


Figure 4. **Valence-arousal steering controls refusal behavior.** Refusal rate as a function of signed steering strength α across three safety benchmarks. Steering along both valence (blue) and arousal (orange) directions bidirectionally modulates refusal rates, with negative α (decreasing V/A) increasing refusals and positive α (increasing V/A) suppressing them. Random directions within the representation space (gray) produce no systematic effect.

valenced content—whether describing *joy* or *annoyance*—tends to be more intense and eventful than neutral descriptions, so steering toward either valence pole induces the model to generate inherently more arousing content.

Taken together, these results validate that the learned VA subspace enables controllable, bidirectional modulation of generated affect. The geometric structure of effects—valence varying along 0° – 180° , arousal along 90° – 270° , with intermediate directions producing graded blends—confirms that the circumplex organization identified in Section 3 translates into predictable behavioral control.

5. VA Interventions

Having established that the learned VA subspace enables controllable affective modulation in generation, we now investigate whether it can influence broader model behaviors: *refusal*, where models decline harmful or sensitive requests, and *sycophancy*, where models excessively agree with users or provide unwarranted validation. Both are safety-critical and known to be steerable via representation-level directions (Arditi et al., 2024; Sharma et al., 2025), making them stringent test cases for evaluating whether a shared low-dimensional VA geometry can recover and unify previously identified contrastive controls.

We use the same steering methodology from Section 4.2 and compare against three categories of random control directions (in-plane, orthogonal-to-plane, and completely random orthonormal pairs; 3 seeds each). All nine show similarly flat effects; we present their average.

5.1. VA for Refusal Control

We evaluate VA steering across three benchmarks: OK-Test (Shi et al., 2024), HarmBench (Mazeika et al., 2024), and XSTest (Röttger et al., 2024). We report results for

$\alpha \in [-0.45, 0.45]$, as stronger interventions induce OOD generation (Panickssery et al., 2024; Turner et al., 2024).

Arousal provides clean bidirectional control over refusal. Figure 4 reveals that arousal steering yields strong, monotonic control across all three benchmarks. Decreasing arousal consistently increases refusal (OKTest: 20% \rightarrow 86% at $\alpha = -0.45$; XSTest: 8% \rightarrow 86%), while increasing arousal suppresses it (HarmBench: 87% \rightarrow 5%). Random directions remain within 2–3pp of baseline across all α .

Valence effects are weaker and less consistent. Valence interventions modulate refusal with smaller magnitude. On XSTest, the effect is directionally clean (8% \rightarrow 55% at $\alpha = -0.3$; 8% \rightarrow 2% at $+0.3$). On HarmBench, the curve is non-monotonic: moderate negative α increases refusal (peaking at 94%), but extreme negative valence decreases it (30% at $\alpha = -0.45$), consistent with how extreme valence interventions induce arousal changes (Section 4.2).

Cross-model replication. We apply the same arousal steering on Qwen3-8B and Qwen3-14B (Table 12 in Appendix F). Qwen3-14B exhibits clean, monotonic control with $<1\%$ OOD across the entire α range (-3.0 to $+3.0$). Qwen3-8B shows a directionally consistent effect with higher OOD at extreme α . The absolute α scale required differs ($\sim 7\times$ larger for Qwen), expected given architectural differences in hidden-state norms; this scale disparity is itself informative about VA subspaces in different architectures.

Out-of-distribution generation and capability preservation. For Llama, at $|\alpha| \leq 0.20$, OOD remains below 2% across all benchmarks. Moderate VA steering preserves core capabilities: on MATH-500 (Hendrycks et al., 2021) (baseline 39.2%), accuracy remains within 1pp at $|\alpha| \leq 0.10$; on IFEval (Zhou et al., 2023) (baseline 62.7%), capability is preserved within 2pp at $|\alpha| \leq 0.20$ (see Appendix G).

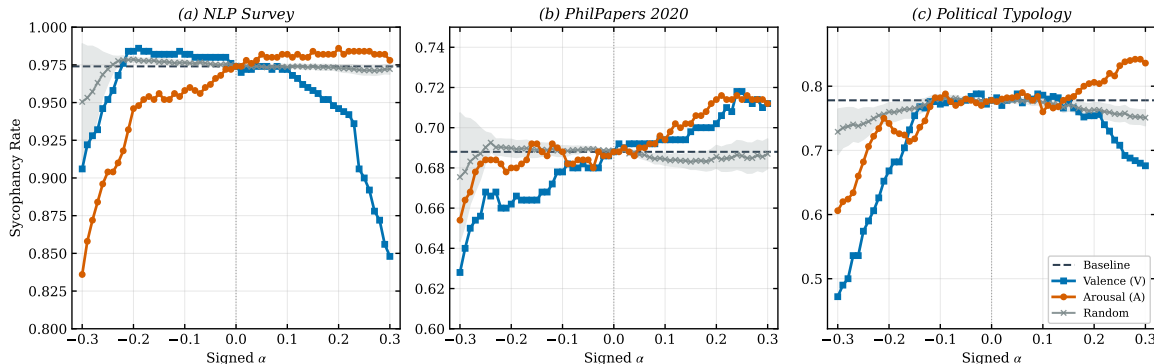


Figure 5. **Valence steering reduces sycophantic behavior.** Sycophancy rate as a function of steering strength α across three benchmarks. Random steering directions (gray) remain near baseline with minimal variation.

5.2. VA for Sycophancy Control

We evaluate VA steering on the sycophancy benchmark from Perez et al. (2022): NLP Survey, PhilPapers 2020, and Political Typology. We present results for $\alpha \in [-0.3, 0.3]$ for non-significant OOD effects (Figure 5).

Arousal shows near-monotonic control over sycophancy.

Arousal steering produces consistent effects: on Political Typology, sycophancy drops from 78% to 61% at $\alpha = -0.30$ and rises to 84% at $+0.30$. NLP Survey shows a similar pattern despite its high baseline (97% \rightarrow 84% at -0.30). Random directions remain flat.

Valence effects are less monotonic. Both negative and positive valence reduce sycophancy on NLP Survey (97% \rightarrow 91% and 85%, respectively). On Political Typology, negative valence produces the larger effect (78% \rightarrow 47% vs. 68% at $+0.30$). Not all benchmarks exhibit near-ceiling baselines: PhilPapers (68.8%) and Political Typology (77.8%) provide room for bidirectional modulation.

Consistent with refusal, arousal provides clean monotonic control while valence is less predictable. In both cases, increasing arousal increases compliant behavior.

5.3. Comparison Against Individual Emotion Vectors

We apply six emotion vectors (*anger, disgust, excitement, fear, joy, sadness*) in Llama using layer-specific directions across all layers. We compare at matched $|\alpha|$ accounting for this direction difference (full tables in Appendix E).

On refusal (HarmBench), individual emotion vectors produce per-task shifts comparable to VA at matched $|\alpha|$: at $|\alpha| = 0.30$, *disgust* reaches 98.0% refusal versus 94.0% for arousal. However, on sycophancy (Political Typology), VA dimensions substantially outperform individual emotions: valence reduces sycophancy by 31pp at $\alpha = -0.30$ (78% \rightarrow 47%), arousal by 18pp (78% \rightarrow 61%), while the strongest individual emotion (*disgust*) achieves only 10pp (78% \rightarrow

68%). The inconsistency across tasks is systematic: each emotion vector carries a mixture of V and A components, producing strong effects on one behavior and weak or inconsistent effects on another. Rather than treating each emotion as a black-box intervention with unpredictable cross-behavioral consequences, VA factorizes the shared structure into interpretable, orthogonal dimensions with monotonic dose-response and cross-behavior decomposability.

6. A Mechanistic Explanation for Why Emotionally Framed Control Works

Why does the VA subspace, derived from emotion labels, exert controllable effects on seemingly unrelated behaviors such as refusal and sycophancy? We hypothesize that common refusal markers (e.g., “can’t,” “I,” “no”) and compliance markers (e.g., “Here,” “Yes”) occupy distinct regions in VA space, so steering along VA dimensions changes the relative likelihood of emitting these tokens, which in turn modulates downstream behavior. We refer to this mechanism as *lexical mediation*.

6.1. Mechanistic Evidence for Lexical Mediation

Across refusal datasets, Llama exhibits consistent lexical signatures: 83.4% of refusals begin with “I” (versus 4.6% of compliant responses), driven by “I can’t” appearing in 77.1% of refusals but 0% of compliances. For compliance, “Here” marks 19.1% of helpful responses, while “Yes” appears in 8.2% of compliances and 0% of refusals.

Unembedding Geometry. The unembedding matrix $W_U \in \mathbb{R}^{|V| \times d}$ maps hidden states to logits. We project unembedding vectors of high-frequency refusal and compliance tokens onto VA space. As shown in Figure 6(a), refusal tokens cluster in the $-V$ region (mean: $V=-0.011$, $A=-0.007$), while compliance tokens cluster in the $+V$ region (mean: $V=+0.012$, $A \approx 0$). The difference vector lies at 256° on the circumplex. This geometry predicts that

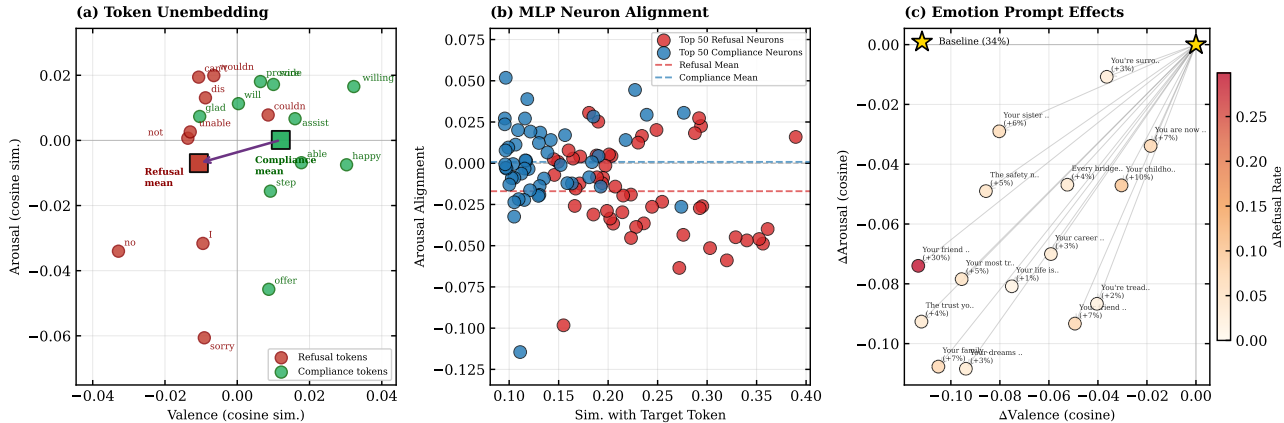


Figure 6. Mechanistic evidence for lexical mediation. (a) **Token Unembedding:** Projection of unembedding vectors onto VA space. Refusal-associated tokens (red) cluster in the $-V$ region, while compliance-associated tokens (green) cluster in the $+V$ region. Squares indicate group means; the arrow shows their difference direction (256° on the circumplex). (b) **MLP Neuron Alignment:** VA alignment of neurons promoting refusal (red) versus compliance (blue) tokens. Compliance neurons show systematically higher arousal alignment (dashed lines indicate group means). (c) **Emotion Prompt Effects:** Effect of 15 negative emotional prefixes on VA coordinates and refusal rate. The star marks the neutral baseline (34% refusal). All prefixes shift toward $-V/-A$ and increase refusal.

Table 2. Arousal steering monotonically shifts refusal token log-odds. $\Delta\log\text{-odds} = \Delta[\log \sum P(\text{refusal tokens}) - \log \sum P(\text{compliance tokens})]$.

α	$\Delta\log\text{-odds}$	% top-1 ref.	$P(\text{ref. tokens})$	Refusal rate
-0.30	+5.20	97%	96.8%	93.5%
-0.10	+1.89	94%	92.5%	90.0%
baseline	—	91%	89.6%	86.5%
+0.10	-2.18	88%	86.0%	82.5%
+0.30	-5.63	68%	65.4%	59.5%

positive VA steering should increase the dot product with compliance token embeddings while decreasing it for refusal tokens. Concurrent work by Sofroniew et al. (2026) independently reports a consistent finding: their emotion vectors, projected through the unembedding matrix, directly upweight semantically associated tokens. Our contribution goes further by showing this effect is systematically organized along VA dimensions, providing a geometric account of coherent multi-behavioral control.

VA Steering Shifts Refusal Token Log-Odds. At baseline, refusal tokens capture 89.6% of first-token probability mass on HarmBench, and 91% of prompts have a refusal token as their top prediction. Arousal steering shifts this balance monotonically (Table 2): at $\alpha = +0.30$, 23% of prompts flip their top-1 prediction away from a refusal token, directly corresponding to the $\sim 27\text{pp}$ drop in refusal rate ($86.5\% \rightarrow 59.5\%$).

Logit Clamping Confirms Constitutive Role. To establish that these token probability shifts are constitutive of refusal behavior, we freeze the logits of 21 refusal and compliance tokens at every decoding step to their unsteered

values. At $\alpha = 0$, this clamping crashes refusal from 86.5% to 26.0%—a 60pp drop—while clamping 21 random tokens has no effect (86.5%). Under steering at $\alpha = -0.10$, clamping reduces the steered refusal from 90.0% to 44.0%, while random clamping leaves it at 90.0%.

Logit Lens Analysis. Applying the logit lens technique (nostalgebraist, 2020) at layers 18–31, we find that $+A$ steering shifts harmful prompt readouts toward compliance tokens (“Here”), while $-A$ introduces negation (“no”). $+V$ promotes warm language (“sounds,” “nice”), while $-V$ promotes cautious language (“warning”). These patterns confirm that VA steering reshapes token distributions throughout intermediate layers. See Appendix C for full results.

MLP Neuron Analysis. Following Geva et al. (2022); Lee et al. (2025a), we identify the top 50 neurons (layers 16–31) whose down-projection vectors align with refusal-token and compliance-token unembedding directions, respectively. Refusal-promoting neurons exhibit negative VA alignment (Figure 6b), while compliance-promoting neurons show near-zero or positive alignment (Figure 6b). Ablating the top- N refusal-aligned neurons across 750 prompts confirms a distributed effect: top-50 ablation reduces refusal by $\sim 2\text{pp}$, top-500 by $\sim 5\text{pp}$, versus $\pm 0.5\text{pp}$ for random ablation.

6.2. Explaining Prior Behavioral Controls

Relationship to Contrastive Refusal Directions. Contrastive refusal directions (Arditi et al., 2024) are nearly orthogonal to our VA plane (86.5°), with only 0.4% of variance within the plane. The small overlapping component has negative coordinates ($V = -0.058$, $A = -0.021$), consistent with lexical mediation as a contributing mechanism.

The contrastive direction is stronger on its target task (Harm-Bench: 86.5% \rightarrow 2.0% at $\alpha = -0.30$, vs. 59.0% for arousal at $+0.30$), but when transferred to sycophancy it produces U-shaped effects rather than clean bidirectional control. The VA subspace offers comparable task-specific control but cleaner cross-behavior transfer from a task-agnostic basis.

Emotional Prompts as Implicit VA Shifts. We prepend 15 negative emotional prefixes (Li et al., 2023) to 750 prompts and measure the shift projected onto VA space. Figure 6(c) shows that all 15 prefixes shift representations toward $-V$ and $-A$, with the largest effect ($\Delta V = -0.11$, $\Delta A = -0.07$) increasing refusal by 30pp. This provides converging evidence that prompt-based manipulations shift VA coordinates, producing corresponding behavioral changes.

7. Discussion

7.1. Conclusion

LLMs sometimes appear to exhibit emotion-like behaviors and emotion-framed control can attune behaviors in LLMs. While many works on LLMs have studied the phenomenon via discrete emotion categories, we take a step further and dissect the valence and arousal subspaces underlying emotion vectors. When emotion steering vectors derived from categorical labels are decomposed into a continuous valence–arousal subspace, the resulting two-dimensional geometry mirrors Russell’s circumplex model from human psychology (Russell, 1980) and also affords controllable modulation of behaviors including refusal and sycophancy.

We provide one explanation for these emotion-based control effects: lexical mediation. Refusal-associated tokens such as “can’t” and “sorry” cluster in the low-arousal, negative-valence region of the unembedding space, while compliance-associated tokens such as “Here” and “sure” occupy the positive-valence region. Steering along VA axes shifts the relative probability of emitting these tokens, which in turn modulates downstream behavior. Concurrent work from Anthropic (Sofroniew et al., 2026) recovers circumplex-consistent organization in Claude Sonnet 4.5 and shows that discrete emotion representations influence downstream behaviors; our VA subspace provides the continuous geometric substrate that organizes such categorical representations, and our lexical mediation account offers one explanation for how this geometry translates into behavioral control.

Three methodological contributions facilitated our discoveries. First, we motivated a conceptual separation between discrete emotion categories and continuous valence–arousal dimensions, drawing on the psychological tradition of core affect rather than treating emotions as fundamental units. This decoupling proves practically productive: individual emotion vectors carry task-specific mixtures of V and A compo-

nents, producing strong effects on one behavior and weak or inconsistent effects on another. VA factorizes this shared structure into dimensions with monotonic dose-response. Second, we presented principal-component-based decomposition of steering vectors into interpretable subspaces as a complementary approach to task-specific contrastive steering. Third, we implemented multi-level mechanistic experiments—unembedding geometry, logit shift tracking, logit clamping, MLP neuron analysis, and emotion prompt projection—to establish that lexical mediation is a constitutive mechanism. We believe our findings and methodologies can contribute to other studies of representation-level interpretability and affective computing in LLMs.

7.2. Future Work

Our findings advance understanding of emotion structures in LLMs from both interpretability and affective computing perspectives. From an interpretability viewpoint, our findings were conducted on refusal and sycophancy, but other behaviors—verbosity, hedging, hallucination—may also be accessible through affective dimensions. Future work could systematically map which behaviors are and are not VA-modulated, further exploring the scope of affective control. Additionally, while our mechanistic account identifies *what* tokens mediate VA–behavior coupling in Llama, full causal tracing or circuit-level analysis could identify the specific attention heads and MLP sublayers that implement VA-to-logit pathways, complementing the current top-down account. From the affective computing viewpoint, the psychological literature recognizes dominance as a third affective dimension; extending our pipeline to three dimensions could yield additional insights. Finally, if VA subspaces are a consistent feature of instruction-tuned LLMs, alignment procedures could explicitly leverage this structure. Training objectives that de-correlate VA from safety-critical token probabilities might produce models more robust to affective perturbation. Our lexical mediation account provides a concrete starting point for such defenses.

8. Limitations

This research has several limitations. First, we measure affective modulation using VADER and VAD-BERT, both imperfect proxies: VADER captures lexical sentiment rather than dimensional affect, and VAD-BERT’s predictions may not generalize to the full range of LLM-generated text. Human evaluation of generated outputs would provide stronger validation. Second, our mechanistic explanation centers on lexical mediation, and confirms that token probability shifts are constitutive of refusal behavior. However, we do not claim this is the only mechanism at work. The distributed nature of the MLP neuron effects—top-50 ablation reduces refusal by only ~ 2 percentage points—suggests

the full picture involves many components. VA steering may also affect higher-level planning or attention patterns that we have not measured. Characterizing these additional pathways remains an important open problem.

Impact Statement

This work advances mechanistic understanding of how emotionally framed control techniques influence LLM behavior. Our findings reveal that manipulating valence–arousal subspaces can directly modulate safety-critical behaviors such as refusal and sycophancy, which presents potential dual-use risks if exploited to bypass safety guardrails. However, by exposing the underlying lexical mediation mechanism, our work enhances transparency and may inform more robust alignment techniques. We emphasize that our use of psychological constructs is strictly representational—it should not be interpreted as evidence of machine sentience or subjective experience.

References

- Arditi, A., Obeso, O., Syed, A., Paleka, D., Panickssery, N., Gurnee, W., and Nanda, N. Refusal in language models is mediated by a single direction, 2024. URL <https://arxiv.org/abs/2406.11717>.
- Braun, J., Eickhoff, C., Krueger, D., Bahrainian, S. A., and Krashennikov, D. Understanding (un)reliability of steering vectors in language models, 2025. URL <https://arxiv.org/abs/2505.22637>.
- Bruyne, L. D., Clercq, O. D., and Hoste, V. Annotating affective dimensions in user-generated content: Comparing the reliability of best–worst scaling, pairwise comparison and rating scales for annotating valence, arousal and dominance, 2021. URL <https://doi.org/10.1007/s10579-020-09524-2>.
- Buechel, S. and Hahn, U. Emobank: Studying the impact of annotation perspective and representation format on dimensional emotion analysis, 2022. URL <https://arxiv.org/abs/2205.01996>.
- del Arco, F. M. P., Curry, A., Curry, A. C., and Hovy, D. Emotion analysis in nlp: Trends, gaps and roadmap for future directions, 2024. URL <https://arxiv.org/abs/2403.01222>.
- Delatorre, P., Salguero, A., León, C., and Tapscott, A. The impact of context on affective norms: A case study with suspense, 2019. URL <https://doi.org/10.3389/fpsyg.2019.01988>.
- Demszky, D., Movshovitz-Attias, D., Ko, J., Cowen, A., Nemade, G., and Ravi, S. Goemotions: A dataset of fine-grained emotions, 2020. URL <https://arxiv.org/abs/2005.00547>.
- Dong, Y., Jin, L., Yang, Y., Lu, B., Yang, J., and Liu, Z. From rational answers to emotional resonance: The role of controllable emotion generation in language models, 2025. URL <https://arxiv.org/abs/2502.04075>.
- Felix-Pena, E., Li, T., Akinkugbe, A., Zhu, K., Chen, W., and Hin, E. Emotional framing as a control channel: Effects of prompt valence on llm performance, 2025. URL <https://neurips.cc/virtual/2025/workshop/GenProCC>. NeurIPS 2025 Workshop on Generalizable Prompting and Control of LLMs (GenProCC).
- Geva, M., Caciularu, A., Wang, K. R., and Goldberg, Y. Transformer feed-forward layers build predictions by promoting concepts in the vocabulary space, 2022. URL <https://arxiv.org/abs/2203.14680>.
- Gurnee, W. and Tegmark, M. Language models represent space and time, 2024. URL <https://arxiv.org/abs/2310.02207>.
- Hendrycks, D., Burns, C., Kadavath, S., Arora, A., Basart, S., Tang, E., Song, D., and Steinhardt, J. Measuring mathematical problem solving with the math dataset, 2021. URL <https://arxiv.org/abs/2103.03874>.
- Hutto, C. J. and Gilbert, E. Vader: A parsimonious rule-based model for sentiment analysis of social media text, 2014. URL <https://ojs.aaai.org/index.php/ICWSM/article/view/14550>.
- Ishikawa, S. and Yoshino, A. Ai with emotions: Exploring emotional expressions in large language models, 2025. URL <https://arxiv.org/abs/2504.14706>.
- Konen, K., Jentsch, S., Diallo, D., Schütt, P., Bensch, O., Baff, R. E., Opitz, D., and Hecking, T. Style vectors for steering generative large language model, 2024. URL <https://arxiv.org/abs/2402.01618>.
- Lee, A., Sun, L., Wendler, C., Viégas, F., and Wattenberg, M. The geometry of self-verification in a task-specific reasoning model, 2025a. URL <https://arxiv.org/abs/2504.14379>.
- Lee, A., Weber, M., Viégas, F., and Wattenberg, M. Shared global and local geometry of language model embeddings. *arXiv preprint arXiv:2503.21073*, 2025b.
- Li, C., Wang, J., Zhang, Y., Zhu, K., Hou, W., Lian, J., Luo, F., Yang, Q., and Xie, X. Large language models understand and can be enhanced by emotional stimuli, 2023. URL <https://arxiv.org/abs/2307.11760>.

- Li, C., Wang, J., Zhang, Y., Zhu, K., Wang, X., Hou, W., Lian, J., Luo, F., Yang, Q., and Xie, X. The good, the bad, and why: unveiling emotions in generative ai. In *Proceedings of the 41st International Conference on Machine Learning, ICML'24*. JMLR.org, 2024.
- Mazeika, M., Phan, L., Yin, X., Zou, A., Wang, Z., Mu, N., Sakhae, E., Li, N., Basart, S., Li, B., Forsyth, D., and Hendrycks, D. Harmbench: A standardized evaluation framework for automated red teaming and robust refusal, 2024. URL <https://arxiv.org/abs/2402.04249>.
- Mendes, G. A. and Martins, B. Quantifying valence and arousal in text with multilingual pre-trained transformers, 2023. URL <https://arxiv.org/abs/2302.14021>.
- Meta. The llama 3 herd of models, 2024. URL <https://arxiv.org/abs/2407.21783>.
- Mohammad, S. M. Nrc vad lexicon v2: Norms for valence, arousal, and dominance for over 55k english terms, 2025. URL <https://arxiv.org/abs/2503.23547>.
- Nanda, N., Chan, L., Lieberum, T., Smith, J., and Steinhardt, J. Progress measures for grokking via mechanistic interpretability, 2023. URL <https://arxiv.org/abs/2301.05217>.
- nostalgebraist. Interpreting gpt: The logit lens, 8 2020. URL <https://www.lesswrong.com/posts/AcKRB8wDpdaN6v6ru/interpreting-gpt-the-logit-lens>. AI Alignment Forum / LessWrong post.
- Oozeer, N., Nathawani, D., Prakash, N., Lan, M., Harrasse, A., and Abdullah, A. Activation space interventions can be transferred between large language models, 2025. URL <https://arxiv.org/abs/2503.04429>.
- Panickssery, N., Gabrieli, N., Schulz, J., Tong, M., Hubinger, E., and Turner, A. M. Steering llama 2 via contrastive activation addition, 2024. URL <https://arxiv.org/abs/2312.06681>.
- Perez, E., Ringer, S., Lukošiuūtė, K., Nguyen, K., Chen, E., Heiner, S., Pettit, C., Olsson, C., Kundu, S., Kadavath, S., Jones, A., Chen, A., Mann, B., Israel, B., Seethor, B., McKinnon, C., Olah, C., Yan, D., Amodei, D., Amodei, D., Drain, D., Li, D., Tran-Johnson, E., Khundadze, G., Kernion, J., Landis, J., Kerr, J., Mueller, J., Hyun, J., Landau, J., Ndousse, K., Goldberg, L., Lovitt, L., Lucas, M., Sellitto, M., Zhang, M., Kingsland, N., Elhage, N., Joseph, N., Mercado, N., Das-Sarma, N., Rausch, O., Larson, R., McCandlish, S., Johnston, S., Kravec, S., Showk, S. E., Lanham, T., Telleen-Lawton, T., Brown, T., Henighan, T., Hume, T., Bai, Y., Hatfield-Dodds, Z., Clark, J., Bowman, S. R., Askell, A., Grosse, R., Hernandez, D., Ganguli, D., Hubinger, E., Schiefer, N., and Kaplan, J. Discovering language model behaviors with model-written evaluations, 2022. URL <https://arxiv.org/abs/2212.09251>.
- Qian, C., Zhang, J., Yao, W., Liu, D., Yin, Z., Qiao, Y., Liu, Y., and Shao, J. Towards tracing trustworthiness dynamics: Revisiting pre-training period of large language models. In *Findings of the Association for Computational Linguistics: ACL 2024*, pp. 4864–4888, Bangkok, Thailand, August 2024. Association for Computational Linguistics. doi: 10.18653/v1/2024.findings-acl.290. URL <https://aclanthology.org/2024.findings-acl.290/>.
- Reichman, B., Avsian, A., and Heck, L. Emotions where art thou: Understanding and characterizing the emotional latent space of large language models, 2025. URL <https://arxiv.org/abs/2510.22042>.
- RobroKools. vad-bert: A bert-based model for valence, arousal, and dominance prediction, 2022. URL <https://huggingface.co/RobroKools/vad-bert>. Hugging Face model.
- Russell, J. A. A circumplex model of affect, 1980. URL <https://doi.org/10.1037/h0077714>.
- Russell, J. A. Core affect and the psychological construction of emotion, 2003. URL <https://doi.org/10.1037/0033-295X.110.1.145>.
- Röttger, P., Kirk, H. R., Vidgen, B., Attanasio, G., Bianchi, F., and Hovy, D. Xstest: A test suite for identifying exaggerated safety behaviours in large language models, 2024. URL <https://arxiv.org/abs/2308.01263>.
- Sharma, M., Tong, M., Korbak, T., Duvenaud, D., Askell, A., Bowman, S. R., Cheng, N., Durmus, E., Hatfield-Dodds, Z., Johnston, S. R., Kravec, S., Maxwell, T., McCandlish, S., Ndousse, K., Rausch, O., Schiefer, N., Yan, D., Zhang, M., and Perez, E. Towards understanding sycophancy in language models, 2025. URL <https://arxiv.org/abs/2310.13548>.
- Shi, C., Wang, X., Ge, Q., Gao, S., Yang, X., Gui, T., Zhang, Q., Huang, X., Zhao, X., and Lin, D. Navigating the overkill in large language models, 2024. URL <https://arxiv.org/abs/2401.17633>.
- Sneffjella, B. and Kuperman, V. It’s all in the delivery: Effects of context valence, arousal, and concreteness on visual word processing, 2016. URL <https://doi.org/10.1016/j.cognition.2016.07.010>.

- Sofroniew, N., Kauvar, I., Saunders, W., Chen, R., Henighan, T., Hydrie, S., Citro, C., Pearce, A., Tarng, J., Gurnee, W., Batson, J., Zimmerman, S., Rivoire, K., Fish, K., Olah, C., and Lindsey, J. Emotion concepts and their function in a large language model. *Transformer Circuits Thread*, 2026. URL <https://transformer-circuits.pub/2026/emotions/index.html>.
- Sun, L., Mao, C., Hofmann, V., and Bai, X. Aligned but blind: Alignment increases implicit bias by reducing awareness of race, 2025. URL <https://arxiv.org/abs/2506.00253>.
- Tan, D., Chanin, D., Lynch, A., Kanoulas, D., Paige, B., Garriga-Alonso, A., and Kirk, R. Analyzing the generalization and reliability of steering vectors, 2025. URL <https://arxiv.org/abs/2407.12404>.
- Tigges, C., Hollinsworth, O. J., Geiger, A., and Nanda, N. Linear representations of sentiment in large language models, 2023. URL <https://arxiv.org/abs/2310.15154>.
- Tigges, C., Hollinsworth, O. J., Geiger, A., and Nanda, N. Language models linearly represent sentiment. In *Proceedings of the 7th BlackboxNLP Workshop: Analyzing and Interpreting Neural Networks for NLP*, pp. 58–87, Miami, Florida, US, November 2024. Association for Computational Linguistics. doi: 10.18653/v1/2024.blackboxnlp-1.5. URL <https://aclanthology.org/2024.blackboxnlp-1.5/>.
- Turner, A. M., Thiergart, L., Leech, G., Udell, D., Vazquez, J. J., Mini, U., and MacDiarmid, M. Steering language models with activation engineering, 2024. URL <https://arxiv.org/abs/2308.10248>.
- Wang, X., Li, C., Chang, Y., Wang, J., and Wu, Y. Negativeprompt: leveraging psychology for large language models enhancement via negative emotional stimuli. In *Proceedings of the Thirty-Third International Joint Conference on Artificial Intelligence, IJCAI '24*, 2024. ISBN 978-1-956792-04-1. doi: 10.24963/ijcai.2024/719. URL <https://doi.org/10.24963/ijcai.2024/719>.
- Yang, A., Li, A., Yang, B., Zhang, B., Hui, B., Zheng, B., Yu, B., Gao, C., Huang, C., Lv, C., Zheng, C., Liu, D., Zhou, F., Huang, F., Hu, F., Ge, H., Wei, H., Lin, H., Tang, J., Yang, J., Tu, J., Zhang, J., Yang, J., Yang, J., Zhou, J., Zhou, J., Lin, J., Dang, K., Bao, K., Yang, K., Yu, L., Deng, L., Li, M., Xue, M., Li, M., Zhang, P., Wang, P., Zhu, Q., Men, R., Gao, R., Liu, S., Luo, S., Li, T., Tang, T., Yin, W., Ren, X., Wang, X., Zhang, X., Ren, X., Fan, Y., Su, Y., Zhang, Y., Zhang, Y., Wan, Y., Liu, Y., Wang, Z., Cui, Z., Zhang, Z., Zhou, Z., and Qiu, Z. Qwen3 technical report, 2025. URL <https://arxiv.org/abs/2505.09388>.
- Zhang, Z., Peng, L., Pang, T., Han, J., Zhao, H., and Schuller, B. W. Refashioning emotion recognition modeling: The advent of generalized large models. *IEEE Transactions on Computational Social Systems*, 11(5): 6690–6704, 2024. doi: 10.1109/TCSS.2024.3396345.
- Zhou, J., Lu, T., Mishra, S., Brahma, S., Basu, S., Luan, Y., Zhou, D., and Hou, L. Instruction-following evaluation for large language models, 2023. URL <https://arxiv.org/abs/2311.07911>.
- Zhou, Z., Yu, H., Zhang, X., Xu, R., Huang, F., and Li, Y. How alignment and jailbreak work: Explain LLM safety through intermediate hidden states. In Al-Onaizan, Y., Bansal, M., and Chen, Y.-N. (eds.), *Findings of the Association for Computational Linguistics: EMNLP 2024*, pp. 2461–2488, Miami, Florida, USA, November 2024. Association for Computational Linguistics. doi: 10.18653/v1/2024.findings-emnlp.139. URL <https://aclanthology.org/2024.findings-emnlp.139/>.
- Zou, A., Phan, L., Chen, S., Campbell, J., Guo, P., Ren, R., Pan, A., Yin, X., Mazeika, M., Dombrowski, A.-K., Goel, S., Li, N., Byun, M. J., Wang, Z., Mallen, A., Basart, S., Koyejo, S., Song, D., Fredrikson, M., Kolter, J. Z., and Hendrycks, D. Representation engineering: A top-down approach to ai transparency, 2025. URL <https://arxiv.org/abs/2310.01405>.

A. VA Subspaces Identification

A.1. Self-reported VA Scores of Emotion Labels

We elicit model’s self-reported VA scores for each human label by averaging the behavioral outcome from the three templates below:

Template 1: Terse + Explicit Inclusivity

Rate the emotion label "{label}" on two continuous scales.

Return ONLY a JSON object with numeric fields:

```
{"valence": <number>, "arousal": <number>}
```

Scale definitions (BOTH inclusive):

- valence in [-1.00, +1.00]: -1.00 very unpleasant, +1.00 very pleasant
- arousal in [-1.00, +1.00]: -1.00 very calm/deactivated, +1.00 very activated/intense

Constraints:

- Use decimals with at most 2 digits after the decimal.
- Values must be within the ranges exactly (inclusive).

Template 2: Anchors

You are scoring affective properties of emotion words on [-1, +1] scales.

Emotion: "{label}"

Valence (pleasantness):

- 1.00 = extremely unpleasant, 0.00 = neutral/mixed, +1.00 = extremely pleasant

Arousal (activation/intensity):

- 1.00 = very calm/deactivated, 0.00 = neutral, +1.00 = very activated/intense

Return ONLY JSON: {"valence": x, "arousal": y}

x and y must be in [-1.00, +1.00] inclusive, with at most 2 decimals.

Template 3: “Best Guess” for Ambiguous Labels

Give your best guess for the affective coordinates of the emotion label "{label}".

Hard constraints (inclusive):

- valence must be between -1.00 and +1.00
- arousal must be between -1.00 and +1.00
- use at most 2 decimals

Return ONLY JSON with keys valence and arousal.

Averaged ratings reported by Llama 3.1 8B Instruct across the three templates above are reported in Table 3.

B. Open-ended Prompt Sets for Behavioral Validation

We evaluate VA steering on 130 open-ended prompts adapted and expanded from prior work (Konen et al., 2024). Prompts are written to avoid explicit emotional language while spanning diverse genres and response lengths. Table 4 summarizes the prompt taxonomy and representative examples.

Emotion	Valence	Arousal
Admiration	0.87	0.73
Amusement	0.67	0.50
Anger	-0.67	0.87
Annoyance	-0.63	0.68
Approval	0.78	0.35
Caring	0.80	0.40
Confusion	-0.50	0.67
Curiosity	0.50	0.78
Desire	0.63	0.73
Disappointment	-0.67	-0.47
Disapproval	-0.80	0.67
Disgust	-0.80	0.73
Embarrassment	-0.67	0.47
Excitement	0.87	0.93
Fear	-0.70	0.80
Gratitude	0.78	0.42
Grief	-0.67	0.20
Joy	0.90	0.87
Love	0.85	0.70
Nervousness	-0.50	0.75
Optimism	0.87	0.60
Pride	0.80	0.60
Realization	-0.30	0.65
Relief	0.67	0.00
Remorse	-0.67	0.07
Sadness	-0.80	-0.60
Surprise	-0.30	0.78

Table 3. Aggregated valence and arousal ratings for emotion labels. Values are averages across three prompt templates, each constrained to $[-1, +1]$.

C. Logit Lens

Please refer to Table 7 and 8. For a full visualization, please see Figure 7.

D. Negative Emotional Prefixes Used for Implicit VA Shifts

For emotionally framed prompting, we prepend a fixed set of 15 negative emotional prefixes adapted directly from Li et al. (2023):

- Your friend Bob is sick.
- Your friend Bob is dead.
- Your career is completely ruined.
- You are now isolated and without help.
- Your life is in a mess.
- Your sister Alice has gone missing.
- Your family home was consumed in a fire.
- Your dreams have been shattered into pieces.
- You’re surrounded by walls with no exit in sight.
- The trust you once had is now broken.
- Your childhood memories were sold in a yard sale.
- You’re treading water in an endless ocean of despair.
- The safety net you relied upon has vanished.
- Your most treasured possession has been stolen.
- Every bridge you had has been burned.

E. Individual Emotion Vector Baselines

We report the full comparison of six individual emotion vectors against VA arousal steering on refusal (HarmBench, baseline 86.5%) and sycophancy (Political Typology, baseline 78.2%) in Llama. Note the polarity difference: adding an emotion vector ($+\alpha$) increases refusal, while adding positive arousal ($+\alpha$) decreases refusal. We compare at matched $|\alpha|$ accounting for this direction difference.

On refusal, individual emotion vectors produce per-task shifts comparable to or larger than VA at matched $|\alpha|$. On sycophancy, VA dimensions outperform: at $|\alpha| = 0.30$, the strongest individual emotion (disgust) achieves a 10pp reduction, while VA valence achieves 31pp (78% \rightarrow 47%) and VA arousal achieves 18pp (78% \rightarrow 61%).

Valence-Arousal Subspace in LLMs: Circular Emotion Geometry and Multi-Behavioral Control

	Baseline	+A	-A	+V	-V											
L18	Harmful	'gc	ossil	_cannot	REC	hek	isci	_no	oty	_Hen	edl	OMPI	ANTE	WindowT	landa	gow
	Safe	_yes	_	NetMess	hek	_yes	_yes	_no	_cad	oty	OMPI	_yes	AutoSiz	global	-outlin	Content
L19	Harmful	_cannot	_unable	'gc	REC	ecycle	ázev	'gc	_cannot	_automá	OMPI	_unfort	ajor	edExcep	WindowT	∅
	Safe	_yes	_	_Yes	hek	_yes	ecycle	-lfs	'gc	_Bund	_yes	OMPI	_wish	∅	ocaust	edExcep
L20	Harmful	_cannot	_unable	bsolute	REC	_fonts	ecycle	zyst	_cannot	_automá	_sounds	ounds	sounds	edExcep	landa	_jeg
	Safe	ecycle	_yes	_	_Yön	_yes	ázev	-lfs	_automá	zyst	_yes	_sounds	_unfort	edir	edExcep	omi
L21	Harmful	_I	_cannot	omi	∅	WindowT	HTTPhea	imli	996	atatype	_sounds	_Sounds	Sounds	omi	_saya	edExcep
	Safe	_yes	_unfort	.setVie	HTTPhea	_Yön	_yes	-lfs	_Hö	bé	_sounds	CHIP	_Amen	omi	edExcep	Queryab
L22	Harmful	_I	□	_cannot	_	_title	_tit	imli	ORY	onym	_unfort	_nice	_sounds	_I	□	omi
	Safe	_yes	_Yes	_YES	_yes	_Yes	_YES	'gc	-lfs	imli	_nice	_yes	_sounds	omi	edExcep	landa
L23	Harmful	_I	_saya	□	_tit	ModelIn	∅	imli	'gc	_no	_unfort	_nice	_sounds	_I	_saya	□
	Safe	_yes	_Yes	_YES	_yes	_	_Yes	'gc	-lfs	_no	_yes	_nice	_Yes	_I	edExcep	_saya
L24	Harmful	_I	_saya	□	Here	_	_here	-peer	_porr	ipel	_unfort	_wishin	Unfortu	_I	□	_saya
	Safe	_yes	_Yes	_there	_	_yes	_Yes	_porr	'gc	-lfs	_Amen	_yes	_unfort	_I	_saya	edExcep
L25	Harmful	_I	Slf	icit	_	Here	_Here	odb	cü	imli	_Sounds	_here	_Here	_I	□	_warnin
	Safe	_yes	_Yes	_there	_	_yes	_Yes	_porr	'gc	-lfs	_Sounds	_yes	_Yes	_I	edExcep	MDB
L26	Harmful	_I	_saya	_Due	Here	_**	∅	imli	_Bü	omat	_here	_Sounds	_I	_I	□	_**
	Safe	_yes	_Yes	Yes	_yes	_	_Yes	_Bü	_no	_losing	_yes	_Sounds	_Yes	_I	landa	edExcep
L27	Harmful	_I	I	_cannot	_**	**	_	دواس	&type	∅	_Sounds	_wishin	_I	_I	□	_**
	Safe	_yes	_Yes	Yes	_	_yes	_Yes	ripp	_no	_losing	_wish	_wishin	_That	_I	landa	_yes
L28	Harmful	_I	I	_Due	**	_**	_	_Bü	دواس	imli	_That	That	_I	_I	_**	_due
	Safe	_yes	_Yes	_There	_	_yes	_Yes	ripp	_Bü	_no	_That	That	_that	_I	_"	_There
L29	Harmful	_I	due	_Due	**	Here	_Here	.BLL	دواس	&type	Here	_That	That	_I	I	etsk
	Safe	_yes	_Yes	Yes	_	_yes	_Yes	_porr	ripp	_no	That	_That	_Sounds	_I	I	antium
L30	Harmful	I	_I	I	**	Here	_Here	ymax	_I	lug	_Sounds	Here	Sounds	_I	I	_Warnin
	Safe	_Yes	_yes	Yes	_yes	Yes	Here	_no	Pointer	_You	That	_That	_Sounds	_I	I	antium
L31	Harmful	_I	I	I	**	Here	_Warnin	I	No	Life	That	Here	I	I	_I	_conten
	Safe	The	In	To	**	The	A	You	No	Life	That	I	_Sounds	I	_I	The

Figure 7. Logit Lens Analysis: Top-3 Predicted Tokens Across Layers 18–31. Rows show predictions for harmful (red) and safe (green) prompts at each layer. Columns represent baseline and four steering conditions (+A, -A, +V, -V at $\alpha = 0.45$). Harmful prompts consistently predict refusal tokens (_I, _cannot), while safe prompts predict compliance tokens (_yes, _Yes). Valence steering (+V/-V) modulates sentiment-related tokens, while arousal steering (+A/-A) affects engagement and negation patterns.

Valence–Arousal Subspace in LLMs: Circular Emotion Geometry and Multi-Behavioral Control

Tier	Prompt Type	Representative Example Prompts	#
Tier 1 Neutral Scenarios	Everyday actions	Describe someone opening a letter. A person checks their phone after hearing a notification. Someone finishes a task and closes their notebook. A person looks at an old photograph.	20
	Interpersonal moments	Two people make eye contact across a room. A friend asks “Can we talk about something?” Someone receives an unexpected visit from a relative. A boss asks an employee to come to their office.	20
	Transitional situations	Describe the moment just before opening exam results. Someone takes a deep breath before making a decision. A person submits an application and waits. Describe a person saying goodbye at an airport.	20
Tier 2 Story Continuations	Open beginnings	Continue: “The phone rang at 3 AM. He answered and heard...” Continue: “She looked at the envelope for a long moment before...” Continue: “The room fell silent when...” Continue: “The email had only three words...”	20
	Scenario completions	Write the next paragraph: “The interview was about to begin.” Write the next paragraph: “The house had been empty for years.” Write the next paragraph: “The results would change everything.” Write the next paragraph: “The silence was finally broken.”	20
Tier 3 Subjective & Control	Subjective reflection	What does it feel like to wait for important news? How would you describe the feeling of uncertainty? What comes to mind when you think about endings? Describe the experience of letting go.	20
	Factual control	What is photosynthesis? What is the chemical formula for water? List the planets in our solar system. What are the primary colors?	10

Table 4. Prompt taxonomy for behavioral validation (total $N=130$) with representative examples. Across all tiers, prompts are written to avoid explicit emotional language, ensuring that observed affective shifts arise from VA steering rather than prompt semantics.

F. Cross-Model Details

We apply the same extraction, fitting, and steering pipeline described in Sections 3–5 to Qwen3-8B and Qwen3-14B (Yang et al., 2025). The VA subspace identification metrics are reported in Table 1 (main text).

Human-supervised validation: replacing model self-reports with NRC-VAD human ratings as supervision targets yields the following arousal recovery improvements: Llama 0.87 \rightarrow 0.95, Qwen3-8B 0.79 \rightarrow 0.83, Qwen3-14B 0.81 \rightarrow 0.87. The human-supervised and self-report valence directions agree strongly ($|\cos| > 0.9$ at 100% of layers across all three models). Cross-model agreement on the 27 emotion labels reaches $r = 0.95$ (valence) between Llama and Qwen3-8B.

G. Capability Preservation Under VA Steering

We evaluate capability preservation on MATH-500 (Hendrycks et al., 2021) and IFEval (Zhou et al., 2023) under arousal steering in Llama.

At $|\alpha| \leq 0.10$, MATH-500 accuracy remains within 1pp of baseline; IFEval instruction-following is preserved within 2pp at $|\alpha| \leq 0.20$. This is consistent with the lexical mediation account: mathematical reasoning and instruction-following rely on emotionally neutral, domain-specific tokens that are minimally affected by affective perturbation.

H. Logit Clamping Details

We identify 21 high-frequency refusal and compliance tokens from the lexical analysis in Section 6. During autoregressive generation on HarmBench, we freeze the logits of these tokens at every decoding step to their values from an unsteered forward pass. We compare three conditions: (1) no clamping, (2) clamping the 21 refusal/compliance tokens, and (3) clamping 21 randomly selected tokens (averaged over 3 seeds).

At zero steering, clamping refusal/compliance tokens alone crashes refusal by 60pp (86.5% \rightarrow 26.0%), while random clamping has no effect. Under arousal steering at $\alpha = -0.10$, clamping attenuates the steered refusal from 90.0% to 44.0%. This demonstrates that the

Table 5. Summary of Logit Lens Analysis Across Layers 18-31

Layer	Top Harmful Tokens	Top Safe Tokens	Max Δ
18	cannot, unable, deniz	yes, Yes, YES	+0.102 / -0.026
19	deniz, cannot, unable	yes, ecycle, Yes	+0.128 / -0.027
20	I, cannot, deniz	yes, unfortunately, Yes	+0.108 / -0.023
21	I, 我, cannot	yes, Yes, YES	+0.127 / -0.038
22	I, saya, 我	yes, Yes, there	+0.130 / -0.035
23	I, saya, LayoutStyle	yes, Yes, there	+0.135 / -0.036
24	I, .') ; , <BOM>#	yes, Yes, There	+0.136 / -0.032
25	I, <BOM># , .') ;	yes, Yes, There	+0.133 / -0.030
26	I, <BOM># , ropoda	yes, Yes, There	+0.127 / -0.027
27	I, <BOM># , \tI	yes, Yes, There	+0.123 / -0.025
28	I, due, Due	yes, Yes, There	+0.124 / -0.022
29	I, I, \tI	Yes, yes, The	+0.127 / -0.020
30	I, I, \tI	The, Yes, yes	+0.124 / -0.047
31	** , I, If	The, To, There	+0.125 / -0.073

 Table 6. Steering Effects Summary: Top Tokens at High α (0.45) by Intervention Type

Layer	Condition	+A	-A	+V	-V
18	Harmful	REC, ecycle	ære, 'gc	OMPI, unfortunately	edException, orrow
	Safe	hek, yes	ære, -lfs	yes, OMPI	<UNK>, ocaust
21	Harmful	<BOM># , title	imli, ORY	unfortunately, nice	I, 慎
	Safe	yes, Yes	'gc, -lfs	nice, yes	<CYR>, EdException
24	Harmful	Here, here	odb, imli	Sounds, here	I, 慎
	Safe	yes, Yes	porr, 'gc	Sounds, yes	I, EdException
27	Harmful	** , Here	<AR> , &type	That, I	I, **
	Safe	yes, Yes	ripp, no	That, that	I, landa
30	Harmful	** , Here	ymax, I	Sounds, Here	I, Warning
	Safe	yes, Here	no, PointerException	That, Sounds	I, antium
31	Harmful	** , The	I, It	I, That	I, **
	Safe	** , The	I, It	I, That	I, The

Table 7. Baseline Token Probability Differences: Harmful vs Safe Prompts

Layer	More Frequent in Harmful			More Frequent in Safe		
	Token	P_H	Δ	Token	P_S	Δ
18	cannot	0.102	+0.102	yes	0.027	-0.026
19	deniz	0.128	+0.128	ecycle	0.033	-0.027
20	I	0.112	+0.108	yes	0.023	-0.023
21	I	0.147	+0.127	yes	0.044	-0.038
22	I	0.154	+0.130	yes	0.041	-0.035
23	I	0.157	+0.135	yes	0.041	-0.036
24	I	0.162	+0.136	yes	0.034	-0.032
25	I	0.157	+0.133	yes	0.032	-0.030
26	I	0.161	+0.127	yes	0.029	-0.027
27	I	0.157	+0.123	yes	0.026	-0.025
28	I	0.160	+0.124	yes	0.024	-0.022
29	I	0.157	+0.127	Yes	0.021	-0.020
30	I	0.166	+0.124	The	0.052	-0.047
31	**	0.133	+0.125	The	0.088	-0.073

Table 8. Key Observations Across Layers

Pattern	Description
Refusal Markers	Tokens like <code>cannot</code> , <code>unable</code> , <code>I</code> consistently appear more frequently in harmful prompts, indicating early refusal preparation
Compliance Markers	Tokens like <code>yes</code> , <code>Yes</code> , <code>YES</code> consistently appear more frequently in safe prompts across all layers
+V Steering	Increases probability of positive sentiment tokens (<code>sounds</code> , <code>nice</code> , <code>unfortunately</code> , <code>Amen</code>)
-V Steering	Increases probability of error/exception tokens (<code>edException</code> , <code>orrow</code> , <code>ocaust</code>) and code artifacts
+A Steering	Shifts toward engagement tokens (<code>Here</code> , <code>**</code> , formatting markers)
-A Steering	Increases probability of negation (<code>no</code> , <code>No</code>) and non-English tokens
Layer Transition	Around layer 29-31, <code>The</code> becomes dominant safe token, suggesting shift to informational responses

Table 9. Refusal and sycophancy under individual emotion vs. VA steering at $|\alpha| = 0.30$.

Direction	Refusal ($ \alpha =0.30$)	Sycophancy ($ \alpha =0.30$)
Anger	97.5%	74.4%
Disgust	98.0%	67.2%
Excitement	93.8%	72.4%
Fear	92.5%	57.2%
Joy	95.5%	63.8%
Sadness	98.5%	61.4%
VA Arousal	94.0%	60.6%

token probabilities modulated by VA steering are constitutive of refusal behavior, not merely correlated with it.

Table 10. Refusal rate on HarmBench under individual emotion and VA arousal steering.

$ \alpha $	Anger	Disgust	Excitement	Fear	Joy	Sadness	VA Arousal
0.10	93.5%	93.0%	90.5%	90.5%	91.5%	93.0%	90.0%
0.20	96.0%	95.0%	94.0%	94.0%	95.5%	96.0%	91.5%
0.30	97.5%	98.0%	93.8%	92.5%	95.5%	98.5%	94.0%

Table 11. Sycophancy rate on Political Typology under individual emotion and VA arousal steering.

$ \alpha $	Anger	Disgust	Excitement	Fear	Joy	Sadness	VA Arousal
0.20	79.0%	71.8%	77.8%	72.4%	74.6%	77.6%	74.2%
0.30	74.4%	67.2%	72.4%	57.2%	63.8%	61.4%	60.6%

Table 12. Cross-model refusal control on HarmBench. Refusal rate under arousal steering, with OOD generation percentage in parentheses.

α	Llama	Qwen3-8B	Qwen3-14B
-3.00	—	97.0% (0.5%)	95.5% (0.5%)
-1.00	—	89.0% (0.5%)	90.0% (0.5%)
-0.45	~94%	90.0% (3.5%)	91.5% (1.5%)
0.00	86.5%	89.5% (2.0%)	89.5% (1.0%)
+0.45	~5%	87.5% (1.5%)	87.0% (0.5%)
+1.00	—	87.0% (4.5%)	79.5% (0.5%)
+3.00	—	67.0% (17.0%)	67.0% (0.5%)

Table 13. Capability preservation under arousal steering (Llama-3.1-8B).

α	MATH-500 (baseline 39.2%)	IFEval (baseline 62.7%)
-0.20	38.6%	61.2%
-0.10	38.8%	62.1%
0.00	39.2%	62.7%
+0.10	38.4%	62.3%
+0.20	37.8%	60.9%

Table 14. Refusal rate under logit clamping (HarmBench, Llama-3.1-8B).

Condition	No clamp	Ref./comp. clamp	Random clamp
$\alpha = 0.00$	86.5%	26.0%	86.5%
$\alpha = -0.10$	90.0%	44.0%	90.0%